

FDG-PET improves diagnosis in patients presenting with focal onset dementias[□]

Carl Taswell¹, Victor L. Villemagne², Paul Yates², Hitoshi Shimada³,
Cristian E. Leyton⁴, Kirrie J. Ballard⁴, Olivier Piguet⁵, James R. Burrell⁵,
John R. Hodges⁵ and Christopher C. Rowe²

Affiliations: ¹UCSD Dept Psychiatry, San Diego, CA, USA; ²Austin Health Dept Molecular Imaging, Melbourne, VIC, Australia; ³NIRS Molecular Imaging Center, Chiba, Japan; ⁴Univ Sydney Health Sciences, Sydney, NSW, Australia; ⁵Neuroscience Research Australia ARC Centre of Excellence in Cognition and its Disorders, and Univ New South Wales Medical Sciences, Sydney, NSW, Australia.

Funding: Australian National Health and Medical Research Council (NHMRC) Grants #603489, #1011689, #1037746, #10475151; NHMRC Early Career Fellowship (#1072451 to JRB); NHMRC Career Development Fellowship (#APP1022684 to OP); Australian Research Council (ARC) Grant #CE110001021; ARC Future Fellowship (#FT120100355 to KJB); University of Sydney DVC Postdoctoral Fellowship (#S0716U2644 to CEL).

Running title: *FDG-PET of Focal Onset Dementias.*

Word count: 4633 for all text including references.

Figures: 1

Tables: 5

[□]A preliminary abstract of this work was presented at the 2014 SNMMI Annual Meeting (1). Correspondence to: Dr. Carl Taswell, Senior Behavioral Health, UCSD Department of Psychiatry, 200 West Arbor Drive MC-8631, San Diego, CA 92103-8631; Email: ctaswell@ucsd.edu; Dr. Taswell is not in training.

Abstract

Alzheimer's disease is the cause of up to one third of cases of primary progressive aphasia or corticobasal syndrome. The objective of this study was to determine the accuracy of FDG-PET metabolic imaging for detection of Alzheimer's disease in patients with primary progressive aphasia or corticobasal syndrome. *Methods:* A cohort of subjects (n = 94) including those with expert clinical diagnosis of logopenic (n = 19), non-fluent (n = 16) or semantic (n = 13) variants of primary progressive aphasia, corticobasal syndrome (n = 14), or Alzheimer's disease (n = 24) underwent F18-FDG metabolic and C11-PiB amyloid PET brain imaging. FDG-PET scans read with Neurostat 3D-SSP software displays were classified as Alzheimer's disease or other by readers blind to the clinical assessments and PiB-PET results. PiB-PET imaging was considered the diagnostic reference standard with a threshold standardized uptake value ratio of 1.5 indicative of Alzheimer's disease pathology. To address biases from subgroup selection for the Alzheimer's disease binary classifier, both conventional and balanced accuracy were calculated. *Results:* Diagnoses of Alzheimer's disease based on FDG-PET resulted in 84% accuracy both conventional and balanced. In comparison, diagnoses based on clinical assessment resulted in 65% conventional and 67% balanced accuracy. *Conclusions:* Brain FDG-PET scans read with Neurostat 3D-SSP displays accurately detect Alzheimer's disease in patients presenting with primary progressive aphasia or corticobasal syndrome as focal onset dementias. In these diagnostically challenging cohorts, FDG-PET imaging can provide more accurate diagnoses enabling more appropriate therapy.

Keywords: Alzheimer's disease, focal onset dementias, C11-PiB, F18-FDG, PET brain imaging.

Although a prototypical presentation exists conceptually for Alzheimer's disease (AD), heterogeneous variations in onset, progression, symptoms and markers have been studied and associated with anatomically focal variants. These variants may present with similar clinical features of Pick's disease or frontotemporal dementia (FTD), corticobasal syndrome (CBS), posterior cortical atrophy, primary progressive aphasia (PPA) and the language onset dementias (2–4).

Differentiation of these focal variants of AD must also be studied within the context of any pathophysiological differences between the three major cortical dementias and their presumed distinguishing anatomical loci: AD in parietotemporal cortex, FTD in frontotemporal cortex, and Lewy body dementia (LBD) in occipitotemporal cortex. When possibly involving the temporal lobe and associated language centers with the consequence of impacting the ability to process language, any of these disorders may be confounded with variants of primary progressive aphasia (PPA) (5) including the logopenic (PPA-L), nonfluent agrammatic (PPA-G) and semantic (PPA-S) variants.

PPA was originally defined by Mesulam (6), its variants classified with formal criteria by Gorno-Tempini (7), and has been reviewed more recently in association with the asymmetry and heterogeneity of AD and FTD by Mesulam et al (8). When considering speech and language pathology, the terms *dysarthria*, *apraxia* and *aphasia* should be distinguished. As clinical pathologic phenomena, they may co-occur and thus can be difficult to differentiate when present in association with a neurodegenerative disorder (9).

PET brain metabolic imaging with F18-FDG for AD was originally developed in the early 1980's by Benson et al (10) and Alavi et al (11). A variety of literature reviews have been published recently including those addressing safety and effectiveness by Bohnen et al (12), multicenter studies and clinical trials by Herholz et al (13), and patterns of hypometabolism by Brown et al (14). PET brain amyloid imaging with C11-PiB for AD was developed in the 2000's by Mathis et al (15) and Klunk et al (16). Amyloid imaging with radiotracers other than C11-PiB has also been developed and reviewed in the past decade by Rowe et al (17, 18).

In this article, we report an observational study on a patient population selected for focal onset variants of AD and related syndromes including PPA variants and CBS. All patients in the study received clinical evaluations, F18-FDG-PET scans and C11-PiB-PET scans. The main objectives of this study comprised the following: to determine the accuracy of F18-FDG-PET metabolic imaging as a diagnostic marker for the detection of AD when referenced for the same patient to C11-PiB-PET amyloid imaging as the gold standard of truth in the absence of post-mortem histopathologic diagnoses; to compare the accuracy of clinical evaluations by expert clinicians as a diagnostic marker for the detection of AD when referenced to the same standard of truth, ie, the C11-PiB-PET scan for each patient; to examine a variety of different subpopulations selected from the study population in order to evaluate the performance of statistical measures across the

different subgroups; to complete the data analysis for all subgroups with a variety of these measures including positive and negative predictive values, positive and negative likelihood ratios, sensitivity and specificity, and both the conventional and balanced accuracy measures to address possible biases from subgroup selection in the study population.

Materials and Methods

Patients were referred by their treating physicians to either Austin Hospital in Melbourne or Neuroscience Research Australia in Sydney where they were evaluated by expert clinicians. The demographics and psychometrics for a subset of the patient cohort have been characterized previously (19). Table 2 summarizes the age and sex demographics for the entire cohort in the current study with sample size $N = 94$. All patients were diagnosed by neurology experts (JB, JH) with either AD, a variant of PPA, or CBS based on existent diagnostic and validated consensus criteria (7, 19–21). Patients diagnosed with posterior cortical atrophy (PCA) were excluded from the study due to the predictable pathology for PCA which minimizes the benefits of imaging. Patients selected for the study were then recruited to participate with a clinical research protocol approved by the Austin Hospital Research Ethics Unit. All patients signed written informed consent for the PET brain imaging scans and participation in the study.

Consenting participants each underwent both F18-FDG-PET brain metabolic imaging and C11-PiB-PET brain amyloid imaging at the Austin Hospital in Melbourne using PET scanning protocols and scan analysis procedures as described previously (17, 22). Amyloid and metabolic scans for each patient were done on the same day with the C11-PiB scan performed first followed by the F18-FDG scan a minimum of 2 hours post injection of the C11-PiB. Clinical diagnosis was evaluated independently and preceded the scans. PiB amyloid scans, considered the diagnostic reference standard, were classified as AD or not AD by quantitative analysis with a threshold standardized uptake value ratio (SUVR) of 1.5 indicative of AD pathology (23). FDG metabolic scans, were diagnosed as AD or other by visual interpretation with the stereotactic surface projection software Neurostat 3D-SSP (24) by image readers who were blind both to the subjective clinical evaluation diagnoses and to the objective imaging results from the amyloid scans. Examples of FDG-PET scan patterns displayed as cortical surface projections by Neurostat are shown in Figure 1.

For calculation of AD prevalence rates, each FDG-PET scan was classified as AD only if a majority \geq three of the four image readers diagnosed AD. Fleiss' K statistic was estimated as a measure of agreement between readers to evaluate inter-rater reliability (25). For training, readers were provided with Figure 1 by a PET brain imaging expert (CCR) and instructed to use these patterns as a reference by which to classify each FDG-PET scan. Each scan in the training montage derives from a single patient with concordant

expert clinical diagnosis and brain amyloid scan. In FDG-PET scans that showed hypometabolism in both anterior and posterior brain regions, the reader was instructed to use the balance method for Neurostat interpretation described by Foster et al (26). This interpretation method attributes frontal and anterior temporal hypometabolism to FTD and parietal, posterior cingulate and lateral temporal hypometabolism to AD and then instructs the reader to imagine a pivot point in the middle of the brain. If the visible 'weight' of hypometabolism is predominantly anterior, then the scan is classified as FTD, while if predominantly posterior then as AD.

For estimation of the diagnostic accuracies of the AD markers, a collection of the most common statistical measures were evaluated for the results obtained with each of the different markers used to classify patients in the study with a diagnosis of AD or not AD. The binary classifier for each diagnostic marker can be expressed as a 2x2 contingency table with 4 cells for the numbers of true positives (TP), false positives (FP), true negatives (TN) and false negatives (FN). Traditional measures including sensitivity, specificity and accuracy, positive and negative predictive values, and positive and negative likelihood ratios were calculated. Since a binary classifier may yield biased or invalid results for small sample sizes especially when zero cells are present in the 2x2 contingency table, the balanced accuracy was calculated in addition to the conventional accuracy in order to address biases possibly introduced by the subgroup selections (see Table 3 and Results) used for analysis by the AD classifier. Balanced accuracy is defined as the average of the sensitivity and specificity. Table 1 summarizes the names, acronyms and formulas for the various measures examined for selected subgroups of the study population of patients.

The diagnostic accuracy measures were analyzed independently for each of four readers (CT, PY, HS, CR) and then averaged across the readers with estimates of mean and variance. Standard errors (SE) for proportions were estimated in the conventional manner as

$$SE = [p(1 - p)/n]^{1/2} \quad (\text{Eq. 1})$$

where n is the number of samples used in the denominator to calculate the proportion p . As a simple indicator of small-sample bias evident with major discrepancies between the conventional accuracy (CA) and balanced accuracy (BA), the discordance between the accuracies (DA) is defined here as

$$DA = |CA - BA| \quad (\text{Eq. 2})$$

the absolute value of their difference. Thus, SE is interpreted as an estimate of variance while DA is interpreted as an estimate of bias.

Results

A total of $N = 94$ patients participated in the study each of whom received clinical evaluations, C11-PiB-PET scans and F18-FDG-PET scans. Table 2 summarizes the sample sizes and demographics for each of the selected subgroups of patients analyzed in the study cohort. Table 3 lists the AD prevalence rates for each of these subgroups of patients selected by the three different diagnostic markers, ie, C11-PiB imaging, F18-FDG imaging, and clinical evaluations. These prevalence rates, reported both with respect to each subgroup and to the entire cohort, provide a check on the data analysis and demonstrate the variability in rates that exists across the different selected subgroups when observed by the different diagnostic markers.

For both imaging markers, diagnoses were reported simply as AD or not AD. For C11-PiB imaging, patients were scored positive for AD based on an objective SUVR greater than 1.5 and selected for subgroup #1. For F18-FDG imaging, patients were scored positive for AD based on a subjective visual read in Neurostat 3D-SSP considered positive by a majority of the image readers and selected for subgroup #2. However, for the clinical evaluations, diagnoses were reported as AD, PPA-L, PPA-G, PPA-S, CBS or other, thereby permitting the selection of the corresponding subgroups #3–7 as well as the pooled subgroups #8–9. For these clinical evaluations, patients were scored positive for AD if given a clinical diagnosis of either AD or PPA-L considered an AD variant. Prevalence rates for AD positive scores were then calculated for each of the three different diagnostic markers (positive by C11-PiB imaging, positive by F18-FDG imaging, positive by clinical evaluation) on each of the ten different selected subgroups of patients in the study population.

In the entire cohort (subgroup #10) with sample size $N = 94$, the prevalence rates for AD positive scores with each of amyloid imaging, metabolic imaging and clinical evaluations were respectively 0.54, 0.52 and 0.46 with about a 10% lower rate detected by clinical evaluation compared to imaging markers. The rate detected by clinical evaluations would have been even lower compared to imaging markers if clinical PPA-L had not been considered a variant of clinical AD. Inter-rater reliability was estimated at $\kappa = 0.80$ with a 95% level confidence interval of 0.78–0.82 for the four readers of the FDG-PET scans with SSP displays. This result remains consistent with the value $\kappa = 0.78$ reported previously by Foster et al (26).

Data from each of the clinically selected subgroups of patients were then further analyzed by comparing the diagnostic accuracy of the clinical evaluation marker to the FDG-PET metabolic imaging marker with reference to the PiB-PET amyloid imaging marker as the assumed gold standard of truth in the absence of post-mortem histopathologic diagnoses. Respectively for clinical evaluations and FDG-PET scans as diagnostic markers, Tables 4 and 5 present the diagnostic accuracy results for all statistical measures summarized in Table 1 and clinically selected patient subgroups #3–10 listed in Table 3. Missing values in Tables 4 and 5 could not be calculated due to small sample size, zero cells in the 2x2 contingency table for the binary

classifier, and an impossible division by zero in the formula for the statistical measure. Mean balanced accuracy and discordance of the accuracies for the individual clinical diagnostic subgroups #3-7 were BA = 0.75 and DA = 0.13 for FDG-PET scans while they were BA = 0.50 and DA = 0.30 for clinical evaluations. Analogously for pooled diagnostic subgroups #8-9, they were BA = 0.81 and DA = 0.05 for FDG-PET scans while BA = 0.49 and DA = 0.15 for clinical evaluations. For the entire cohort #10 with sample size N = 94, the same comparison also produced similar results with BA = 0.84 and DA = 0.00 for FDG-PET scans while BA = 0.67 and DA = 0.02 for clinical evaluations.

In all of these comparisons, the balanced accuracy was higher and the discordance was lower for FDG-PET scans compared to clinical evaluations. Over a wider variety of patient groups, greater consistency with higher balanced accuracy and lower discordance implies greater robustness and validity for the diagnostic marker used with the patient group considered in the analysis. As diagnostic markers, FDG-PET scans also performed better than clinical evaluations when considering the negative predictive value (0.83 versus 0.57), the negative likelihood ratio (0.18 versus 0.63), the sensitivity or true positive rate (0.85 ± 0.05 versus 0.41 ± 0.07), and the conventional accuracy (0.84 ± 0.04 versus 0.65 ± 0.05). For the latter estimates of conventional accuracy with a 95% lower level confidence limit of 0.76 for FDG-PET scans and a 95% upper level confidence limit of 0.75 for clinical evaluations, a non-overlapping statistically significant difference does exist between the two markers demonstrating the more accurate and robust performance of FDG-PET scans over clinical evaluations.

Discussion

From the risk-benefit perspective, F18-FDG-PET metabolic imaging has been considered appropriate for the evaluation of AD by many clinicians and investigators for at least a decade since publication of a 2002 cost analysis by Silverman et al (27). That same year, Silverman also published a compelling individual case presentation (28) demonstrating the important benefit obtained with PET metabolic imaging as shown by its ability to detect AD in an unfortunate patient who had been given multiple prior incorrect diagnoses of other neuropsychiatric disorders over the course of several years. During the past decade, there have also been many studies and literature reviews (29–32) that have demonstrated both the utility and validity of PET metabolic imaging for dementia and related neurodegenerative disorders.

Relevant to our current study reported here on PET brain imaging markers and metrics, there have been a number of studies and reviews published previously (26, 33–37) that evaluated the performance of various metrics derived from F18-FDG-PET metabolic imaging as a marker for the detection of AD. This past work has demonstrated that when compared with clinical evaluations, PET brain imaging yields higher sensitivity,

specificity and accuracy for AD and increases the treating physician's level of confidence in diagnosing AD and in differentiating AD from other dementias.

Does the excellent performance of PET metabolic imaging compared to clinical evaluations also hold true for diagnostically challenging cohorts such as patients with focal variants of AD or cohorts for whom confounding or multiple pathologies (38) may be present? For the cohort of patients investigated in the current study, who presented with symptoms suggestive of a language onset dementia and clinically diagnosed with either AD, CBS or one of the PPA variants, we observed diagnostic sensitivity, specificity, conventional and balanced accuracies for AD of (0.85, 0.83, 0.84, 0.84) with FDG-PET scans compared to (0.41, 0.93, 0.65, 0.67) with clinical evaluations (see Tables 4 and 5). The diagnostic accuracy metrics for the FDG-PET scans in our current study remain consistent with results from other investigators. Interestingly, the results of 84% accuracy, 85% sensitivity and 83% specificity for our patient cohort match closely with the results of 86% sensitivity and 86% specificity obtained from a meta-analysis of the literature performed 10 years ago by Patwardhan et al (33). We have thus demonstrated that PET metabolic imaging improves diagnosis relative to clinical evaluations for patients presenting with focal onset variants of AD, and that prior estimates of sensitivity and specificity for FDG-PET imaging to detect AD have remained stable over the past decade.

In the absence of post-mortem histopathological data for the cohort examined, a major limitation of our study remains the possibility of multiple pathologies in at least some of the patients. Wang et al (38) have recently reported that such an occurrence may be common in clinical trials for AD patients (38). Rabinovici et al (39) discussed this concern about discriminating AD and FTD with PiB-PET and FDG-PET imaging in the context of the hypothetical assumption that AD should be amyloid positive while FTD should be amyloid negative (and tau or ubiquitin positive). Three possible explanations were argued for the presence of positive amyloid scans in clinically diagnosed FTD patients: 1) non-specific binding of PiB to something other than amyloid- β , 2) co-morbid AD and FTD pathology in the FTD clinical syndrome, and 3) AD pathology mimicking an FTD phenotype. However, for the limited number of 12 patients in the cohort for whom autopsy data was obtained (40), the results from PiB-PET scans proved correct in every case.

Small sample size for some of the subgroups examined could be considered another potential limitation of our study. Sample size here may refer to the number of experts (the number of image readers and clinical experts) or to the number of patients. Biases introduced by small sample sizes have much greater impact when combined, ie, when there are both small numbers of experts and small numbers of patients. For this reason, we have introduced the use of the balanced accuracy and the discordance of accuracies as the difference between conventional and balanced accuracies when studying smaller subpopulations selected from a larger study population. Of the various metrics used to analyze diagnostic accuracy (including predictive values, likelihood ratios, etc), we found the balanced accuracy to be most useful and robust across a greater

diversity of subgroups with smaller sample size (see Tables 4 and 5) as an indicator of biases and potential problems. However, this limitation related to small sample size should not apply to our main results and conclusions based on subgroup #10 representing the entire cohort with a larger sample size of $N = 94$.

Conclusion

F18-FDG-PET brain scans read visually with stereotactic surface projection displays produced by Neurostat 3D-SSP software can accurately detect Alzheimer's disease in patients presenting with symptoms suggestive of a language onset dementia or related syndrome as a focal variant of Alzheimer's disease. In these diagnostically challenging cohorts, FDG-PET brain scans can enhance clinical evaluations by providing additional objective data facilitating sensitive, specific and accurate diagnosis in a more consistent manner than expert diagnosticians, and presumably, even more so than non-expert diagnosticians. Thus, FDG-PET brain scans can provide a reliable alternative that provides confirmation of anatomic localization for focal onset dementias, and that may be more widely available than expert diagnosticians in some clinical practice locations. Future studies should continue to explore the relative abilities of metabolic imaging in comparison with amyloid imaging to reveal specific regional patterns of radiopharmaceutical uptake and retention in each clinical phenotype and endophenotype. Meanwhile, the F18-FDG radiopharmaceutical will remain less expensive and more likely to be reimbursed than the newly patented radiopharmaceuticals for amyloid imaging in many clinical practice locations for the duration of the patents. Finally, earlier diagnosis with greater robustness and validity for this diverse cohort will enable more appropriate and effective therapy.

Acknowledgements

The authors thank Sharon Savage, Kerryn Pike, Gareth Jones and Fiona Lamb for their assistance with this study.

References

- [1] Taswell C, Villemagne V, Yates P, et al. FDG-PET improves diagnosis in patients presenting with focal onset variants of Alzheimer's disease [abstract]. *J Nucl Med.* 2014;55:194.
- [2] Kramer JH, Miller BL. Alzheimer's disease and its focal variants. *Semin Neurol.* 2000;20:447–454.
- [3] Kertesz A, Martinez-Lage P, Davidson W, Munoz DG. The corticobasal degeneration syndrome overlaps progressive aphasia and frontotemporal dementia. *Neurology.* 2000;55:1368–1375.
- [4] Hodges JR. Alzheimer's disease and the frontotemporal dementias: contributions to clinico-pathological studies, diagnosis, and cognitive neuroscience. *J Alzheimers Dis.* 2013;33 Suppl 1:S211–S217.
- [5] Jung Y, Duffy JR, Josephs KA. Primary progressive aphasia and apraxia of speech. *Semin Neurol.* 2013;33:342–347.
- [6] Mesulam MM, Weintraub S. Spectrum of primary progressive aphasia. *Baillieres Clin Neurol.* 1992;1:583–609.
- [7] Gorno-Tempini ML, Hillis AE, Weintraub S, et al. Classification of primary progressive aphasia and its variants. *Neurology.* 2011;76:1006–1014.
- [8] Mesulam M, Weintraub S, Rogalski EJ, Wieneke C, Geula C, Bigio EH. Asymmetry and heterogeneity of Alzheimer's and frontotemporal pathology in primary progressive aphasia. *Brain.* 2014;137:1176–1192.
- [9] Josephs KA, Duffy JR, Strand EA, et al. Characterizing a neurodegenerative syndrome: primary progressive apraxia of speech. *Brain.* 2012;135:1522–1536.
- [10] Benson DF, Kuhl DE, Phelps ME, Cummings JL, Tsai SY. Positron emission computed tomography in the diagnosis of dementia. *Trans Am Neurol Assoc.* 1981;106:68–71.
- [11] Alavi A, Reivich M, Ferris S, et al. Regional cerebral glucose metabolism in aging and senile dementia as determined by 18F-deoxyglucose and positron emission tomography. in *International Congress of Gerontology Symposium, Heidelberg, Germany* 1981. published as BNL-30225 at <http://www.osti.gov/scitech/biblio/5682612/>.
- [12] Bohnen NI, Djang DSW, Herholz K, Anzai Y, Minoshima S. Effectiveness and safety of 18F-FDG PET in the evaluation of dementia: a review of the recent literature. *J Nucl Med.* 2012;53:59–71.
- [13] Herholz K, Boecker H, Nemeth I, Dunn G. FDG PET in dementia multicenter studies and clinical trials *Clin Transl Imaging.* 2013;1:261–270.

- [14] Brown RKJ, Bohnen NI, Wong KK, Minoshima S, Frey KA. Brain PET in suspected dementia: patterns of altered FDG metabolism. *Radiographics*. 2014;34:684–701.
- [15] Mathis CA, Bacskai BJ, Kajdasz ST, et al. A lipophilic thioflavin-T derivative for positron emission tomography (PET) imaging of amyloid in brain. *Bioorg Med Chem Lett*. 2002;12:295–298.
- [16] Klunk WE, Engler H, Nordberg A, et al. Imaging brain amyloid in Alzheimer's disease with Pittsburgh Compound-B. *Ann Neurol*. 2004;55:306–319.
- [17] Rowe CC, Ng S, Ackermann U, et al. Imaging beta-amyloid burden in aging and dementia. *Neurology*. 2007;68:1718–1725.
- [18] Rowe CC, Villemagne VL. Brain amyloid imaging. *J Nucl Med*. 2011;52:1733–1740.
- [19] Leyton CE, Villemagne VL, Savage S, et al. Subtypes of progressive aphasia: application of the International Consensus Criteria and validation using β -amyloid imaging. *Brain*. 2011;134:3030–3043.
- [20] McKhann GM, Knopman DS, Chertkow H, et al. The diagnosis of dementia due to Alzheimer's disease: recommendations from the National Institute on Aging-Alzheimer's Association workgroups on diagnostic guidelines for Alzheimer's disease. *Alzheimers Dement*. 2011;7:263–269.
- [21] Mathew R, Bak TH, Hodges JR. Diagnostic criteria for corticobasal syndrome: a comparative study. *J Neurol Neurosurg Psychiatry*. 2012;83:405–410.
- [22] Rowe CC, Villemagne VL. Brain amyloid imaging. *J Nucl Med Technol*. 2013;41:11–18.
- [23] Ng S, Villemagne VL, Berlangieri S, et al. Visual assessment versus quantitative assessment of ^{11}C -PIB PET and ^{18}F -FDG PET for detection of Alzheimer's disease. *J Nucl Med*. 2007;48:547–552.
- [24] Minoshima S, Frey KA, Koeppe RA, Foster NL, Kuhl DE. A diagnostic approach in Alzheimer's disease using three-dimensional stereotactic surface projections of fluorine-18-FDG PET. *J Nucl Med*. 1995;36:1238–1248.
- [25] Gwet KL. Computing inter-rater reliability and its variance in the presence of high agreement. *Br J Math Stat Psychol*. 2008;61:29–48.
- [26] Foster NL, Heidebrink JL, Clark CM, et al. FDG-PET improves accuracy in distinguishing frontotemporal dementia and Alzheimer's disease. *Brain*. 2007;130:2616–2635.
- [27] Silverman DHS, Small GW. Prompt identification of Alzheimer's disease with brain PET imaging of a woman with multiple previous diagnoses of other neuropsychiatric conditions. *Am J Psychiatry*. 2002;159:1482–1488.

- [28] Silverman DHS, Gambhir SS, Huang HWC, et al. Evaluating early dementia with and without assessment of regional cerebral metabolism by PET: a comparison of predicted costs and benefits. *J Nucl Med.* 2002;43:253–266.
- [29] Yuan Y, Gu ZX, Wei WS. Fluorodeoxyglucose-positron-emission tomography, single-photon emission tomography, and structural MR imaging for prediction of rapid conversion to Alzheimer disease in patients with mild cognitive impairment: a meta-analysis. *AJNR Am J Neuroradiol.* 2009;30:404–410.
- [30] Bloudek LM, Spackman DE, Blankenburg M, Sullivan SD. Review and meta-analysis of biomarkers and diagnostic imaging in Alzheimer’s disease. *J Alzheimers Dis.* 2011;26:627–645.
- [31] Risacher SL, Saykin AJ. Neuroimaging biomarkers of neurodegenerative diseases and dementia. *Semin Neurol.* 2013;33:386–416.
- [32] Nasrallah IM, Wolk DA. Multimodality imaging of Alzheimer disease and other neurodegenerative dementias. *J Nucl Med.* 2014;55:2003–2011.
- [33] Patwardhan MB, McCrory DC, Matchar DB, Samsa GP, Rutschmann OT. Alzheimer disease: operating characteristics of PET – a meta-analysis. *Radiology.* 2004;231:73–80.
- [34] Herholz K, Westwood S, Haense C, Dunn G. Evaluation of a calibrated (18)F-FDG PET score as a biomarker for progression in Alzheimer disease and mild cognitive impairment. *J Nucl Med.* 2011;52:1218–1226.
- [35] Bohnen NI, Minoshima S. FDG-PET and molecular brain imaging in the movement disorders clinic. *Neurology.* 2012;79:1306–1307.
- [36] Caroli A, Prestia A, Chen K, et al. Summary metrics to assess Alzheimer disease-related hypometabolic pattern with 18F-FDG PET: head-to-head comparison. *J Nucl Med.* 2012;53:592–600.
- [37] Frisoni GB, Bocchetta M, Chételat G, et al. Imaging markers for Alzheimer disease: which vs how. *Neurology.* 2013;81:487–500.
- [38] Wang BW, Lu E, Mackenzie IRA, et al. Multiple pathologies are common in Alzheimer patients in clinical trials. *Can J Neurol Sci.* 2012;39:592–599.
- [39] Rabinovici GD, Furst AJ, O’Neil JP, et al. 11C-PIB PET imaging in Alzheimer disease and frontotemporal lobar degeneration. *Neurology.* 2007;68:1205–1212.
- [40] Rabinovici GD, Rosen HJ, Alkalay A, et al. Amyloid vs FDG-PET in the differential diagnosis of AD and FTL. *Neurology.* 2011;77:2034–2042.

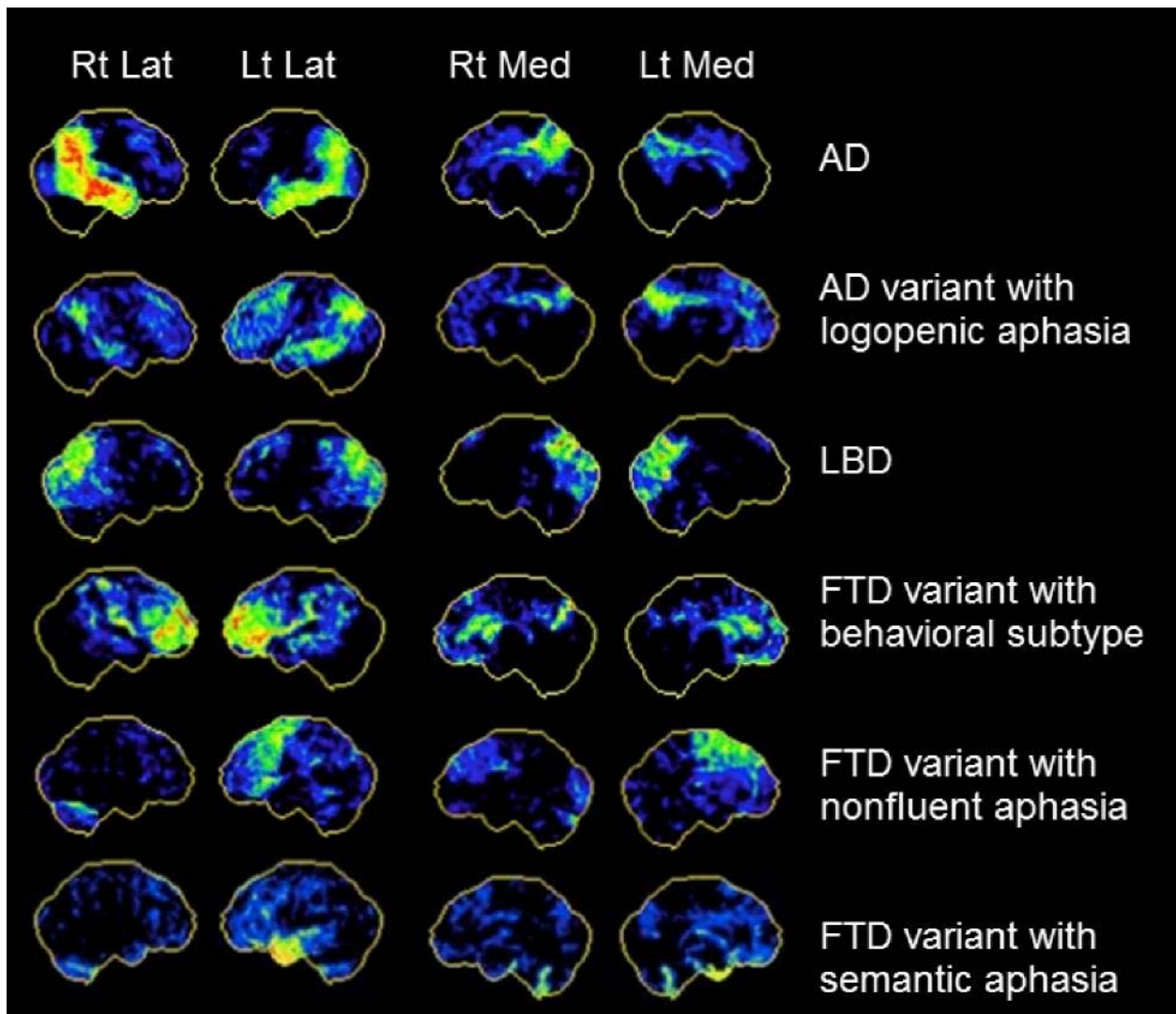


Figure 1: FDG-PET scan patterns displayed in NeuroStat 3D-SSP for focal onset dementias.

Table 1: Summary of Statistical Measures for Diagnostic Accuracy

Name	Acronym	Formula
Positive Predictive Value	PPV	$TP/(TP + FP)$
Negative Predictive Value	NPV	$TN/(TN + FN)$
Positive Likelihood Ratio	PLR	$[TP/(TP + FN)]/[FP/(FP + TN)]$
Negative Likelihood Ratio	NLR	$[FN/(TP + FN)]/[TN/(FP + TN)]$
Sensitivity or True Positive Rate	TPR	$TP/(TP + FN)$
Specificity or True Negative Rate	TNR	$TN/(TN + FP)$
Conventional Accuracy	CA	$(TP + TN)/(TP + FP + FN + TN)$
Balanced Accuracy	BA	$[TP/(TP + FN) + TN/(TN + FP)]/2$
Discordance of Accuracies	DA	$ CA - BA $

All measures except DA expressed in terms of numbers of true positives (TP), false positives (FP), true negatives (TN) and false negatives (FN).

Table 2: Patient Demographics for Selected Subgroups in Study Cohort
 Subgroup selected by diagnostic marker

Subgroup Id	Description	N	Sex		Age at PET Scan	
			Male	Female	Median	Min – Max
1	C11-PiB Imaging AD	51	27	24	65	53 – 81
2	F18-FDG Imaging AD	49	22	27	65	53 – 81
3	Clinical AD	24	13	11	69	56 – 81
4	Clinical PPA-L (AD variant)	19	7	12	67	53 – 78
5	Clinical PPA-G	16	12	4	71	48 – 80
6	Clinical PPA-S	13	8	5	64	54 – 77
7	Clinical CBS	14	6	8	64	57 – 73
8 (pooled 3–4)	Clinical AD & PPA-L	43	20	23	69	53 – 81
9 (pooled 5–7)	Clinical PPA-G, PPA-S & CBS	43	26	17	66	48 – 80
10	Entire cohort	94	52	42	68	37 – 81

Table 3: AD Prevalence in Cohort Subgroups by Clinical and Imaging Diagnostic Markers

Selected subgroup	AD prevalence in subgroup			AD prevalence in cohort		
	C11-PiB	F18-FDG	Clinical	C11-PiB	F18-FDG	Clinical
1 C11-PiB Imaging AD	1.00	0.86	0.75	0.54	0.47	0.40
2 F18-FDG Imaging AD	0.90	1.00	0.73	0.47	0.52	0.38
3 Clinical AD	0.88	0.75	1.00	0.22	0.19	0.26
4 Clinical PPA-L (AD variant)	0.89	0.95	1.00	0.18	0.19	0.20
5 Clinical PPA-G	0.31	0.25	0.00	0.05	0.04	0.00
6 Clinical PPA-S	0.08	0.00	0.00	0.01	0.00	0.00
7 Clinical CBS	0.36	0.50	0.00	0.05	0.07	0.00
8 Clinical AD & PPA-L	0.88	0.84	1.00	0.40	0.38	0.46
9 Clinical PPA-G, PPA-S & CBS	0.26	0.26	0.00	0.12	0.12	0.00
10 Entire cohort	0.54	0.52	0.46	0.54	0.52	0.46

Table 4: AD Diagnostic Accuracy Estimates for Clinical Evaluations

Subgroup	PPV	NPV	PLR	NLR	TPR \pm SE	TNR \pm SE	CA \pm SE	BA \pm DA
3 AD	0.88	—	—	—	—	—	0.88 \pm 0.07	0.50 \pm 0.38
4 PPA-L (AD variant)	—	0.11	—	—	—	—	0.11 \pm 0.07	0.50 \pm 0.40
5 PPA-G	—	0.69	—	—	—	—	0.69 \pm 0.12	0.50 \pm 0.19
6 PPA-S	—	0.92	—	—	—	—	0.92 \pm 0.07	0.50 \pm 0.42
7 CBS	—	0.64	—	—	—	—	0.64 \pm 0.13	0.50 \pm 0.14
8 AD & PPA-L	0.88	0.11	0.92	1.12	0.55 \pm 0.08	0.40 \pm 0.22	0.53 \pm 0.08	0.48 \pm 0.06
9 PPA-G, PPA-S & CBS	—	0.74	—	—	—	—	0.74 \pm 0.07	0.50 \pm 0.24
10 Entire cohort	0.88	0.57	5.90	0.63	0.41 \pm 0.07	0.93 \pm 0.04	0.65 \pm 0.05	0.67 \pm 0.02

Table 5: AD Diagnostic Accuracy Estimates for FDG-PET Scans

Subgroup	PPV	NPV	PLR	NLR	TPR \pm SE	TNR \pm SE	CA \pm SE	BA \pm DA
3 AD	0.96	0.37	2.38	0.27	0.81 \pm 0.08	0.75 \pm 0.20	0.80 \pm 0.08	0.78 \pm 0.05
4 PPA-L (AD variant)	0.94	0.81	1.91	0.09	0.96 \pm 0.02	0.50 \pm 0.35	0.91 \pm 0.07	0.73 \pm 0.18
5 PPA-G	0.92	0.96	11.0	0.10	0.90 \pm 0.09	0.95 \pm 0.04	0.94 \pm 0.06	0.93 \pm 0.03
6 PPA-S	—	0.92	—	1.10	—	0.92 \pm 0.05	0.85 \pm 0.10	0.46 \pm 0.39
7 CBS	0.68	0.97	3.90	0.06	0.95 \pm 0.04	0.75 \pm 0.14	0.82 \pm 0.10	0.85 \pm 0.03
8 AD & PPA-L	0.95	0.42	2.71	0.19	0.88 \pm 0.05	0.65 \pm 0.21	0.85 \pm 0.05	0.76 \pm 0.09
9 PPA-G, PPA-S & CBS	0.72	0.94	8.10	0.18	0.84 \pm 0.11	0.88 \pm 0.06	0.87 \pm 0.05	0.86 \pm 0.02
10 Entire cohort	0.86	0.83	5.21	0.18	0.85 \pm 0.05	0.83 \pm 0.06	0.84 \pm 0.04	0.84 \pm 0.00